03

High-temperature evaporation of water droplets with solid impurities

© M.S. Schakhray[1,2], D.V. Antonov[1,2], P.A. Strizhak[1,2], S.S. Sazhin[1–3]

[1] Tomsk Polytechnic University, Tomsk, Russi
[2] Kutateladze Institute of Thermophysics, Siberian Branch, Russian Academy of Sciences, Novosibirsk, Russia
[3] School of Architecture, Technology and Engineering, Advanced Engineering Centre, University of Brighton, Brighton, U.K.
E-mail: dva14@tpu.ru

Received September 13, 2024
Revised October 11, 2024
Accepted October 11, 2024

Theoretically predicted characteristics of high-temperature evaporation of water droplets with solid impurities are presented. The evolution of droplet radii and temperatures during evaporation in a heated gas for their initial radii in the range 10 to 100 μm and gas temperatures in the range 500 to 1100 K is investigated. It is shown that an increase in the initial mass fraction of solid impurities in water droplets leads to non-linear increase in their evaporation rate. It is found that for the initial mass fractions of solid impurities in the range 5 to 8%, droplet initial radii in the range 10 to 100 μm and gas temperatures in the range 500 to 1100 K, droplet evaporation times increase from 0.1 to 0.36 s. These times are typical for spraying of wastewater in heating chambers.

Keywords: droplet, evaporation, impurities, heating, thermal purification.

DOI: 10.61011/TPL.2025.02.60633.20119

The lack of clean drinking water is a pressing global issue [1]. In recent years, this problem has become more complicated due to biological attacks and terrorist actions aimed at contaminating water bodies [2], as well as due to the rise in industrial activities accompanied by the production of process water and wastewater. This has a negative impact on the environment and requires enhancement of the existing methods of liquid treatment [3]. Treatment of contaminated and waste water is usually performed in several stages: multistage filtration [4], chemical neutralization of impurities [5], thermal (high-temperature) treatment [6]. Thermal purification methods include evaporation (concentration of impurities), drying (spraying of liquids in a hot air or flue gases), thermal oxidation (burning of combustible impurities). Burning is used to neutralize organic impurities in wastewater. Evaporation [7] is most often used to treat mineralized water. The mineral and solid impurities can be removed from water in two stages i.e. by concentration and dry product extraction. The separation of the dry product can take place, for example, in a spray dryer [8]. The second stage is often replaced by burial of concentrated solutions [9]. The choice of a particular method depends on the volume of wastewater, its composition, calorific value, corrosivity, cost-effectiveness of the process, and the requirements for the treated water. The reason for the limited applicability of thermal methods for treating liquids is that they are expensive and energy intensive, since much energy is required to intensify phase transitions and oxidation reactions [10]. Currently, thermal treatment is used to neutralize wastewater with small relative mass concentrations of solid insoluble impurities (up to 8%) [11]. Typical theoretical evaporation times of sprayed contaminated and waste water are analyzed in this paper. It will allow setting out requirements to optimize liquid spraying taking into account reactor capabilities, liquid composition, thermal conditions, intensification of steam formation by combined methods, application of excessive discharged heat at stations, closed cycle systems using the treated liquid as a working body and heat exchange agent. These issues motivated our research.

Using the model of heat and mass transfer, validated by comparison with experimental data, to analyze the processes of drying and fragmentation of droplets [12,13] we studied high-temperature evaporation of water droplets with solid insoluble impurities. Carbonaceous particles approximated solid insoluble impurities using coal as an example. These impurities fall into process and waste waters during coal preparation. The main thermophysical properties of the components used in the study are summarized in the table. The scientific novelty of the study is to establish functional relationships between the integral characteristics of evaporation of water with solid insoluble impurities and the main input parameters.

Solid impurities dispersed in the vaporizing liquid (water) are considered as non-evaporating component of the droplet. Sedimentation and agglomeration effects characteristic of these impurities are not considered. The droplets are assumed to have a spherical shape. The physical model of high-temperature evaporation of water droplets with solid insoluble impurities is presented in Fig. 1. At the first stage, the droplet is monotonically heated and evaporates. At the initial stage, a homogeneous distribution of particles over the volume is assumed. At the second stage, the concentration of solid insoluble impurities increases near the droplet surface leading to a decrease in mass fraction of water in this region. At the third stage, the heterogeneous

Basic thermophysical characteristics of water droplets and solid insoluble impurities (temperature T in K) [14]

Parameter	Component	
	Distilled water	Insoluble impurity (coal)
Density, kg/m^3	$325 \cdot 0.27^{-\left[1-\left(T/647.096\right)\right]^{0.23}}$	$0.003(T-273.15)^2$ $-1.4065(T-273.15)+1402.9$
Specific heat capacity, J/(kg·K)	$(-2.2417 \cdot 10^4 + 876.97T - 2.5704T^2$ $+2.4838 \cdot 10^{-3} \cdot T^3)/18$	$1154(T-273.15)^{0.0346}$
Thermal conductivity, W/(m·K)	$-0.35667 + 5.057 \cdot 10^{-3} \cdot T - 6.1071 \cdot 10^{-6} \cdot T^2$	$0.0000009(T-273.15)^2$ $-0.0006(T-273.15)+0.2707$
Heat of vaporization, J/kg	$-2.4324 \cdot 10^3 \cdot T + 3.1672 \cdot 10^6$	–
Pressure of saturated vapor, Pa	$8 \cdot 10^{-4} \cdot \exp(0.0508T)$	–
Dynamic viscosity, mPa·s	$3 \cdot 10^{-12} \cdot T^4 - 3.94 \cdot 10^{-9} \cdot T^3 + 2.0328 \cdot 10^{-6} \cdot T^2$ $-4.6803 \cdot 10^{-4} \cdot T + 0.0406389$	–

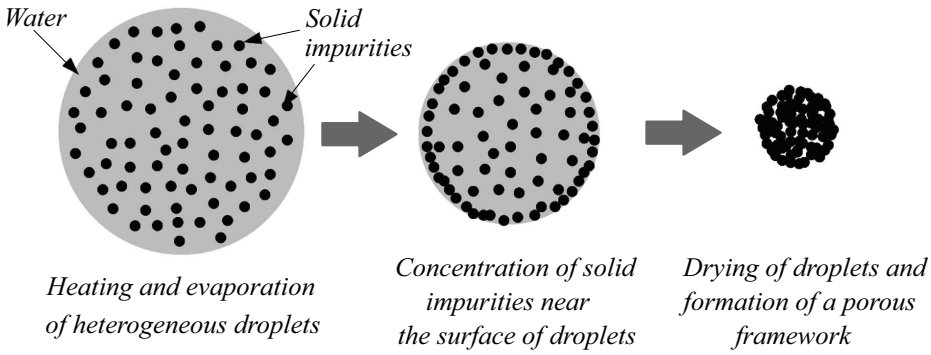

Figure 1. A physical model of high-temperature evaporation of water droplets with solid insoluble impurities.

droplet heating process ends with drying of the droplet and formation of a porous shell. The initial temperature of water droplets in all calculations was taken as $T_{d0} = 300$ K. The initial droplet radii varied in the range of $10-100\,\mu$m, the temperature of the gas medium in the solution region — 500−1100 K, the relative mass fraction of solid insoluble impurities — 5−8%.

The heating process of a water droplet with solid insoluble impurities was described by a transient differential equation of thermal conductivity in a spherical coordinate system

$$\frac{\partial T}{\partial t} = \kappa\left(\frac{\partial^2 T}{\partial R^2} + \frac{2}{R}\frac{\partial T}{\partial R}\right) + P(t, R), \tag{1}$$

where $\kappa = k/(c\rho)$, k, c and ρ — thermal diffusivity, thermal conductivity, specific heat capacity and density, respectively, of water with solid insoluble impurities, R — distance from the droplet center, T — temperature, t — time, $P(t, R)$ — additional heat source (e.g., heating due to thermal radiation).

Initial and boundary conditions are the following

$$T(t=0) = T_{d0}(R), \tag{2}$$

$$h(T_{eff} - T_s) = k\left.\frac{\partial T}{\partial R}\right|_{R=R_d-0}, \tag{3}$$

where $h = \text{const}$ for a short time step — heat transfer coefficient, T_s — droplet surface temperature,

$$T_{eff} = T_g + \frac{\rho L \dot{R}_{d(e)}}{h}, \quad \dot{R}_{d(e)} = \frac{|\dot{m}_d|}{4\pi\rho R_d^2}, \tag{4}$$

L — heat of water vaporization.

The Abramzon and Sirignano [15] model was used to estimate the mass evaporation rate $\dot{m}_d$ and the heat transfer coefficient h:

$$|\dot{m}_d| = 2\pi R_d D_v \rho_{total} \ln(1 + B_M), \tag{5}$$

where D_v — water vapor diffusion coefficient, ρ_{total} — vapor-gas mixture density, B_M — Spalding mass transfer number.

The following equation of diffusion of droplet components in a spherical coordinate system was used:

$$\frac{\partial Y_i}{\partial t} = D\left(\frac{\partial^2 Y_i}{\partial R^2} + \frac{2}{R}\frac{\partial Y_i}{\partial R}\right), \tag{6}$$

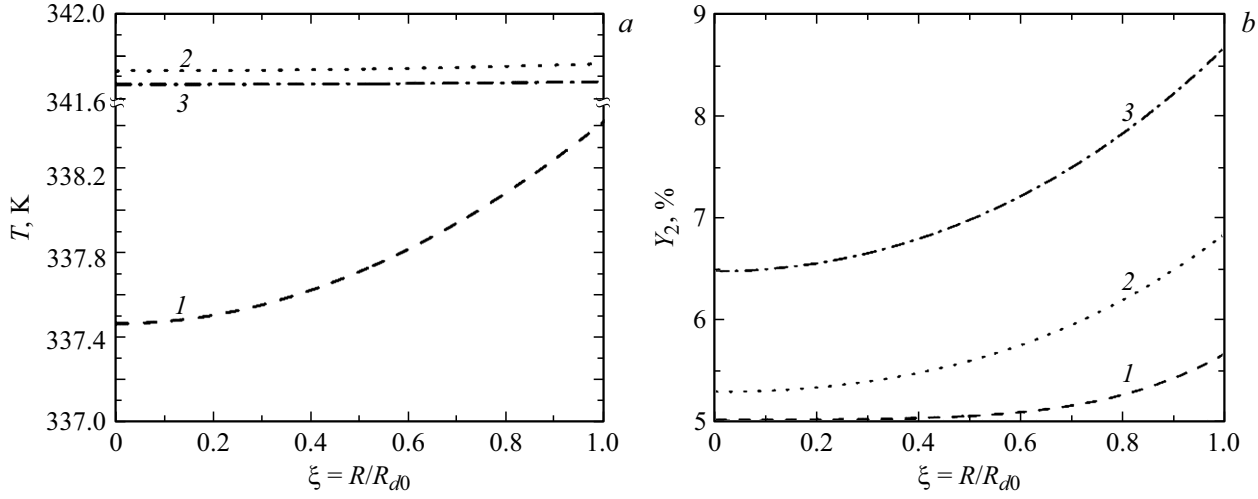

Figure 2. Typical distributions of temperature (a) and mass fractions of solid particles (b) at various time instants for the initial mass fraction of 5%, $T_g = 800$ K and $R_{d0} = 50\,\mu$m at $t = 0.04$ (*1*), 0.08 (*2*) and 0.12 s (*3*).

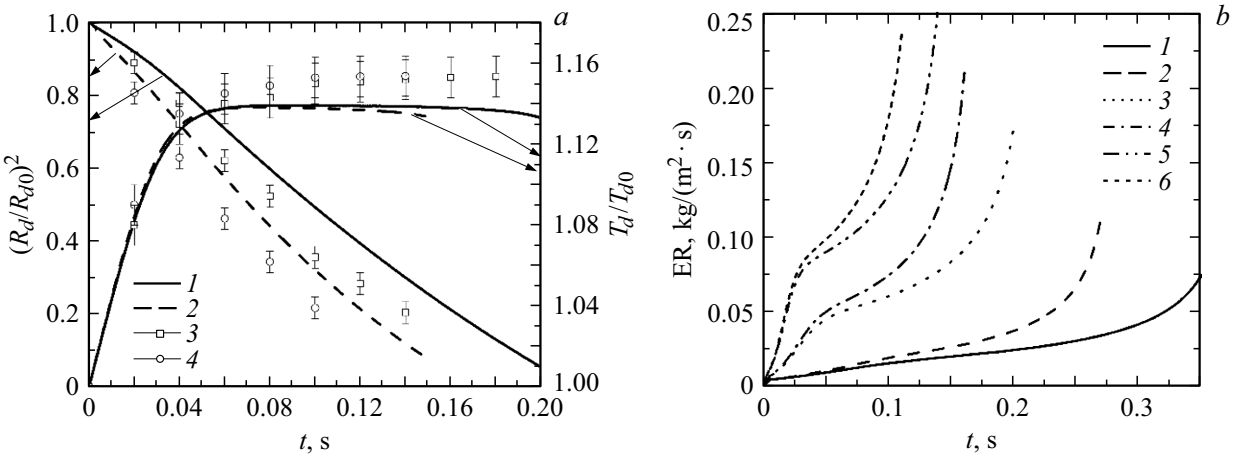

Figure 3. a — typical dynamics of normalized droplet radii squared $(R_d/R_{d0})^2$ and their mean temperatures T_d/T_{d0} for the initial mass fractions of solids 5 % (*1*) and 8% (*2*) at $T_g = 800$ K and $R_{d0} = 50\,\mu$m. Symbols — experimental data for the initial relative mass fractions of solids 5% (*3*) and 8% (*4*). b — predicted evaporation rates (ER) of droplets ($R_{d0} = 50\,\mu$m) with the initial mass fractions of solid particles of 5 (*1, 3, 5*) and 8% (*2, 4, 6*) at $T_g = 500$ (*1, 2*), 800 (*3, 4*) and 1100 K (*5, 6*).

where D — diffusion coefficient of solid insoluble particles in water, Y_i — mass fraction of the i-th component, i — component number ($i = 1$ — water, $i = 2$ — solid insoluble particles.

Initial and boundary conditions:

$$Y_i(t = 0) = Y_{i0}(R), \tag{7}$$

$$\alpha(\varepsilon_i - Y_{is}) = -D\frac{\partial Y_i}{\partial R}\bigg|_{R=R_d-0}, \quad \alpha = \frac{|\dot{m}_d|}{4\pi\rho R_d^2}, \quad \varepsilon_i = \frac{Y_{vis}}{\Sigma_i Y_{vis}}, \tag{8}$$

where Y_{is} — relative mass fractions of the$i$-th component on the surface of a water droplet with solid insoluble impurities, Y_{vis} — mass fraction of the i-th vapor component.

The partial vapor pressure of water $p_v$was determined by Raoul's law

$$p_v = X_{ls}\,p_v^{sat}, \tag{9}$$

where X_{ls} — molar fraction of water on the droplet surface, p_v^{sat} — saturated water vapor pressure.

The values of the thermophysical properties of a water with solid insoluble particles were determined by the following expressions [12]:

$$\rho = \left[\sum_{i=1}^{i=2}(Y_i/\rho_i)\right]^{-1}, \quad c = \sum_{i=1}^{i=2}(Y_i c_i),$$

$$k = \left[\sum_{i=1}^{i=2}(Y_i k_i^{-2})\right]^{-1/2}, \tag{10}$$

where ρ_i, $c_i$and k_i — the density, specific heat capacity and thermal conductivity of water and solid insoluble particles.

The system of equations under consideration is solved analytically, and the analytical solutions are implemented in

the numerical code at each short time step. A constant time step of 10^{-6} s was used. Computer characteristics: Intel(R) Xeon(R) CPU E5-2697 v3 @ 2.60 GHz (number of processors 2), installed RAM 128 GB. Computation time is from 1 to 5 min.

Fig. 2 shows typical distributions of temperature and solid impurity concentration at three time instants ($t = 0.04$, 0.08, 0.12 s) at the initial mass fraction of 5%, $T_g = 800$ K and $R_{d0} = 50\,\mu$m. Note that the highest temperatures within the droplets are predicted near their surface, and the lowest ones — in the center at each time step. Similar conclusions can be drawn for the mass fraction distributions of solid particles: their maximal values are predicted near the droplet surface, and the minimal — in the center. Note that the temperature gradients inside the droplets are low (less than 0.02 K/μm), which indicates the possibility of simplifying the calculation by excluding the heat transfer equation inside droplets from the system of equations under consideration. The gradients of of mass fractions of solid particles, however, cannot be be ignored.

Figure 3, *a* shows the typical dynamics of normalized droplet radii squared, $(R_d/R_{d0})^2$, and their average normalized temperatures, T_d/T_{d0}, for initial mass fractions of solids of 5% (curves *1*) and 8% (curves *2*) at $T_g = 800$ K and $R_{d0} = 50\,\mu$m. One can clearly see in this figure that the higher the mass fraction of solids in water, the more intensive are the processes of their heating and vaporization. For example, when the initial mass fraction of solids increases from 5 to 8%, the time of their evaporation decreases by more than 25%. This is mainly due to an increase in the effective thermal diffusivity in the heterogeneous droplet and therefore an increase in the mass transfer. Note that the final modeling results refer to the time instant of droplet self-conservation due to the formation of a shell of solid particles around water in the droplets. Experimental data are shown by symbols (*3* — 5%, *4* — 8%). These experiments for heating and vaporization of water droplets with solids were carried out using the same setup as in [13] (heat transfer is driven mainly by convection). This setup is the closest to real conditions in the devises for thermal and combustion cleaning of liquids from unregulated impurities [6,7]. The characteristics of the processes of heating and vaporization of water droplets with solid insoluble impurities were recorded using a high-speed video camera Phantom Miro C110 (915 frames per second at a resolution of 1280 by 1024 pixels). The video frames obtained from the experiments were processed using Phantom Camera Control software. The dynamics of droplet size and temperature were recorded. The droplet temperature was measured using a thermocouple (type *K*). The systematic errors of droplet size and temperature registration did not exceed 0.05 mm and 3 K, respectively. When comparing the results of modeling and experiments, higher rates of heating and evaporation of inhomogeneous droplets in experiments (up to 20−30%) should be noted. This is mainly due to the fact that the model did not consider the recirculation of convective flows, as well as sedimentation and agglomeration of solid particles.

Fig. 3, *b* shows the calculated values of evaporation rate (ER) of water droplets ($R_{d0} = 50\,\mu$m) with solid particles with initial mass fractions of 5% and 8% at $T_g = 500$, 800 and 1100 K. As can be seen from the results of simulations, the evaporation rate increases when the mass fraction of solid particles increases following approximately the power law.

Thus, the evaporation time is expected to be in the range 0.1 to 0.36 s for initial mass fractions of soliude in the range 5% to 8%, droplet radii in the range 10 to 100 μm and ambient gas temperatures in the range 800 to 1100 K. This time is sufficient for heating of droplets in chambers for thermal and combustion purification of liquids from unregulated impurities [14]. Thus, the model can predict conditions of water purification at various initial mass fractions of solid insoluble impurities.

Funding

The research was supported by the Ministry of Science and Higher Education of the Russian Federation (grant 075-15-2025-007).

Conflict of interest

The authors declare that they have no conflict of interest.

References

[1] T.A. Karyukhina, I.N. Churbanova, *Khimiya vody i Microbiologiya* (Stroyizdat, M., 1983), p. 123. (in Russian)
[2] A. Zahoor, G. Mao, X. Jia, X. Xiao, J.L. Chen, Environ. Sci.: Adv., **1** (2), 92 (2022). DOI: 10.1039/D2VA00002D
[3] J.A.C. Castellar, A. Torrens, G. Buttiglieri, H. Monclús, C.A. Arias, P.N. Carvalho, A. Galvao, J. Comas, J. Clean. Prod., **340**, 130660 (2022). DOI: 10.1016/j.jclepro.2022.130660
[4] V.A. Nikashina, Sorbtsyonnye i khromatographicheskie protsessy, **19** (3), 289 (2019). (in Russian) DOI: 10.17308/sorpchrom.2019.19/746
[5] D. Ghazi, Z. Rasheed, E. Yousif, Arch. Org. Inorg. Chem. Sci., **3** (3), 344 (2018). DOI: 10.32474/AOICS.2018.03.000161
[6] A. Kizgin, D. Schmidt, A. Joss, J. Hollender, E. Morgenroth, C. Kienle, M. Langer, J. Environ. Manage., **347**, 119001 (2023). DOI: 10.1016/j.jenvman.2023.119001
[7] D.V. Antonov, R.S. Volkov, M.V. Piskunov, P.A. Strizhak, Tech. Phys. Lett., **42** (3), 248 (2016). DOI: 10.1134/S1063785016030032.
[8] D.L. Dubovets, Ecologiya na predpriyatii, № 5 (143), 27 (2023). (in Russian)
[9] B.S. Valiev, D.V. Ivanov, R.R. Shagidullin, Ros. zhurn. prikladnoy ecologii, № 4, 52 (2020). (in Russian) DOI: 10.24411/2411-7374-2020-10034
[10] A.P. Gus'kov, Tech. Phys. Lett., **47**, 553 (2021). DOI: 10.1134/S1063785021060080.

[11] V. Balaram, L. Copia, U.S. Kumar, J. Miller, S. Chidambaram, Geosyst. Geoenviron., **2** (4), 100210 (2023). DOI: 10.1016/j.geogeo.2023.100210
[12] S.S. Sazhin, O. Rybdylova, A.S. Pannala, S. Somavarapu, S.K. Zaripov, Int. J. Heat Mass Transfer, **122**, 451 (2018). DOI: 10.1016/j.ijheatmasstransfer.2018.01.094
[13] D.V. Antonov, G.V. Kuznetsov, P.A. Strizhak, Appl. Therm. Eng., **195**, 117190 (2021). DOI: 10.1016/j.applthermaleng.2021.117190
[14] C.L. Yaws, *Yaws' handbook of thermodynamic and physical properties of chemical compounds* (Knovel, 2003).
[15] B. Abramzon, W.A. Sirignano, Int. Commun. Heat Mass Transfer, **32** (9), 1605 (1989). DOI: 10.1016/0017-9310(89)90043-4

Translated by J.Savelyeva